

**W. Dmochowski**

Institute of Fluid Flow Machinery,  
Polish Academy of Sciences,  
80-952 Gdansk,  
Poland

**K. Brockwell**

Tribology and Mechanics Laboratory,  
National Research Council,  
Vancouver, B.C., V6S 2L2  
Canada

**S. DeCamillo**

**A. Mikula**

Kingsbury, Inc.,  
Philadelphia, PA 19154

# A Study of the Thermal Characteristics of the Leading Edge Groove and Conventional Tilting Pad Journal Bearings

*In this paper dealing with the tilting pad journal bearing, experimental results are presented which show that, at higher shaft speeds, the leading-edge-groove (LEG) design has significantly lower operating temperatures to those of the conventional design of tilting pad journal bearing. Subsequent theoretical analysis has shown that this reduction in pad operating temperature is the result of feeding cool oil directly to the leading edge of the pad. This has the effect of reducing the amount of hot oil carried over from one pad to the next.*

## Introduction

The leading-edge-groove (LEG) bearing is a term used to describe a new design of tilting pad bearing that incorporates an oil distribution groove at the leading edge of each pad. The principle behind the operation of this bearing is that a controlled amount of cool lubricant is introduced directly into the oil film from the groove. In high speed thrust bearings, this method of oil supply has been found to give significantly reduced frictional losses and operating temperatures (Mikula, 1988).

This paper describes an experimental and theoretical study of a leading-edge-groove tilting pad journal bearing. Test results from this bearing are compared with experimental data taken from a conventional tilting pad journal bearing. Initial results are encouraging since they show that the LEG bearing has significantly lower metal temperatures to those of the conventional bearing, when operating at higher shaft speeds. A theoretical study of the LEG bearing indicates that this is the result of reducing the amount of hot oil carried over from one pad to the next.

Hot oil carry over, and the problem of calculating the temperature at the leading edge of the oil film, has been investigated only a few times in recent years. In a series of studies on hot oil carry over in thrust bearings, Ettles (1968, 1970) analyzed the thermal and velocity boundary layers in the space (or groove) between the bearing pads and defined a hot oil carry over factor:

$$\lambda = \frac{t_1 - t_i}{t_j - t_i} \quad (1)$$

From results presented in these papers, it was shown that a layer of hot oil adheres to the thrust runner, regardless of oil flow and temperature conditions within the groove. Providing both the hot oil carry over factor and the runner temperature are known, the temperature of the oil film at the leading edge ( $t_1$ ) can be found. Values of  $\lambda$  vary between 0.5 and 0.93, and were determined experimentally by Ettles (1970), and later by Ettles and Advani (1980).

Using the Ettles' hot oil carry over factor, Vohr (1981) analyzed the behavior of a large thrust bearing, but found that a small inaccuracy in the assumed value of  $\lambda$  could lead to a large difference in the calculated oil temperature. Vohr then considered the heat balance of the entire bearing and included the analysis of the thermal boundary layer across the groove. However, the complexity of this analysis makes its application to the calculation of bearing performance difficult.

Mitsui et al. (1983) presented a modified form of Ettles' hot oil carry over factor that was related to both the outlet flow and the total flow entering the oil film, i.e.,

$$\lambda = \frac{(t_1 - t_i)q_1}{(t_2 - t_i)q_2} \quad (2)$$

The values of  $\lambda$ , estimated experimentally, ranged from 0.4 to 1.0.

Heshmat and Pinkus (1986) considered the energy balance in the bearing groove and obtained the following relationships for calculating the leading edge oil temperature:

$$t_1 = \frac{(q_1 - q_2)t_i + q_2 t_2 - A}{q_1(1 + \lambda)} \quad (3)$$

where

Contributed by the Tribology Division for publication in the JOURNAL OF TRIBOLOGY. Manuscript received by the Tribology Division February 26, 1992; revised manuscript received August 1992. Associate Technical Editor: M. J. Braun.

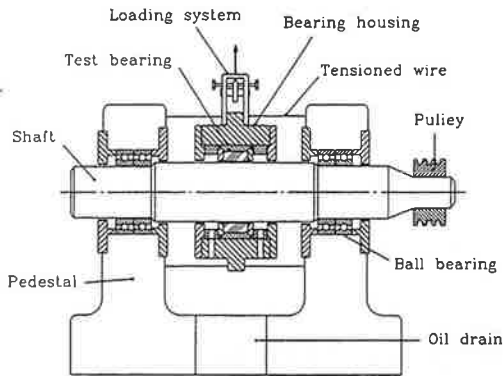


Fig. 1 Schematic of the shaft-bearing assembly

$$A = \begin{cases} 0 & \text{if } t \text{ expressed in } ^\circ\text{F} \\ \frac{160}{9} \lambda q_1 & \text{if } t \text{ expressed in } ^\circ\text{C} \end{cases} \quad (4)$$

The factor  $\lambda$  is referred to as a mixing coefficient and represents the amount of heat lost by the trailing edge oil flow ( $q_2$ ), before entering the leading edge of the next pad. The mixing coefficient was calculated from the following empirical formula:

$$\lambda = 9 \cdot 10^{-3} (1 - 1.017 \bar{U} + 0.017 \bar{U}^2) (5 - 3 \bar{t}_h) \quad (5)$$

where

$$\bar{U} = \frac{U}{5000} \quad (U \text{ in ft/min}) \quad (6)$$

$$\bar{t}_h = \frac{t_h}{120} \quad (t_h \text{ in } ^\circ\text{F}) \quad (7)$$

In this paper dealing with the LEG and conventional designs of tilting pad journal bearing, it is shown that simple "mixing" equations can be used to determine the oil temperature at the leading edge of the pads.

## Experimental Apparatus

**Test Rig.** Figure 1 shows the test arrangement which is based on the concept of a free test bearing and a fixed shaft. In this configuration, the shaft element rotates and the other element (the bearing) moves in response to the applied load.

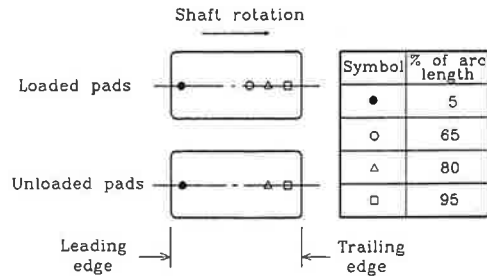


Fig. 2 Location of the thermocouples in the bearing pads

The 0.098 m diameter shaft is supported on high precision, angular contact ball bearings, lubricated by an oil-air system. A 37 kW variable speed electric motor, driving through a belt and pulley system, provides a range of shaft speeds between 1800 and 16500 rev/min.

Eddy current probes mounted on the ends of the bearing housing measure horizontal and vertical displacements of the bearing with respect to the shaft. Nonparallel lateral movement of the bearing, resulting from misalignment of the bearing loading system, is minimized by the use of axial tensioned wires attached to the ends of the bearing housing. Because these wires have lateral flexibility, they have little influence on the radial movement of the bearing housing.

Figure 2 shows where the copper-constantan thermocouples were located in the test bearings. In this arrangement, which was common to both the LEG and conventional bearings, the thermocouples were embedded in the babbitt lining to within 0.5 mm of the bearing surface.

Data from the instrumentation was processed by a high speed data acquisition system. These data were stored in the memory of the data acquisition system and passed, at a later time, to the host computer. Uncertainties in the measurement of temperature, shaft rotational speed, load, and thermocouple location were estimated to be  $\pm 1\text{C}$ ,  $\pm 0.6$  percent,  $\pm 0.9$  percent, and  $\pm 0.5$  mm, respectively.

**Bearing Design and Test Parameters.** The test bearings had a length/diameter ratio of 0.387, and comprised of five offset pivot (0.6), steel backed, babbitt lined pads, a steel aligning ring and two aluminum alloy end plates. The back of each journal pad was contoured both circumferentially and axially to allow the pads to adjust to conditions of axial misalignment. Bearing and pad radial clearances, and pad preload factor, were, respectively, 0.076 mm, 0.102 mm, and 0.25.

## Nomenclature

$c$  = specific heat of oil  
 $d$  = nominal bearing diameter  
 $g$  = local pad thickness  
 $g_{\text{piv}}$  = pad thickness at pivot  
 $h$  = oil film height  
 $k_p$  = heat conductivity of bearing  
 $k_{\text{ol}}$  = heat conductivity of oil  
 $m_b$  = bending moment  
 $p$  = pressure  
 $q_1$  = pad leading edge flow  
 $q_2$  = pad trailing edge flow  
 $r$  = bearing radial coordinate  
 $t_a$  = ambient temperature  
 $t_j$  = journal surface temperature

$t_f$  = oil film temperature  
 $t_i$  = inlet oil temperature  
 $t_l$  = oil temperature at pad leading edge  
 $t_p$  = bearing temperature  
 $u$  = oil velocity in circumferential direction  
 $w$  = oil velocity in axial direction  
 $y_f$  = radial coordinate  
 $z$  = axial coordinate  
 $C$  = pad radial clearance  
 $D$  = assumed pad outside diameter  
 $E$  = modulus of elasticity in tension  
 $G$  = modulus of elasticity in shear

$H$  = nondimensional oil film thickness,  $H = h/C$   
 $I_{\text{piv}}$  = second moment of pad cross section at pivot  
 $I_{\text{piv}} = g_{\text{piv}}^3 L / 12$   
 $L$  = bearing width  
 $M$  = nondimensional viscosity,  $M = \mu / \mu_i$   
 $M_b$  = nondimensional bending moment  $M_b = m_b A (2C/d)^2 / (\mu_i \omega L d)$   
 $\text{Nu}$  = Nusselt number,  $\text{Nu} = \alpha (d/2) / k_p$   
 $P$  = nondimensional pressure,  $P = p (2C/d)^2 / (\mu_i \omega)$   
 $R$  = nondimensional radius,  $R = 2r/d$

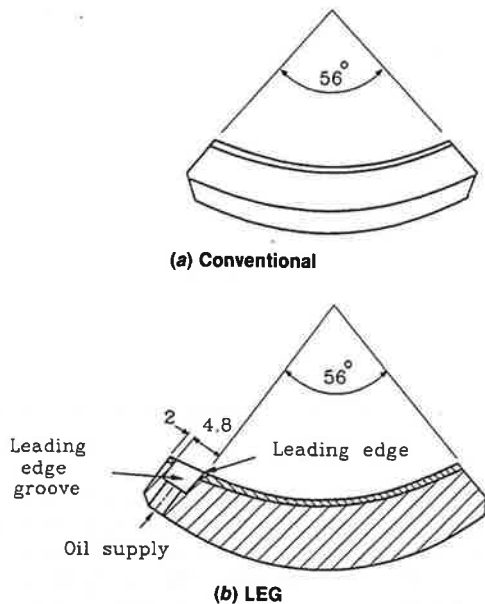


Fig. 3 Pad arrangements

Figure 3 shows the arrangement of the conventional and LEG bearing pads. The effective pad angle of both bearings was 56.1 deg, although the LEG pad was slightly longer because of the leading edge groove. The axial length of this groove was 33.5 mm.

The lubricant was a light turbine oil (ISO VG32) with a viscosity of 0.02325 Pa.s @ 40C and 0.0054 Pa.s @ 100C. The oil supply temperature to the test bearings was regulated between 48C and 50C by a feedback control device and a shell and tube heat exchanger.

The bearings were tested for two directions of load, viz.: load between pads (LBP) and load on pad (LOP). Other test conditions were as follows:

- Shaft speeds: 1800 to 16500 rev/min.
- Bearing loads: 5.2 and 11.2 kN.
- Nominal oil flow rates: dependent on load and speed (see Table 1)

Tests were also conducted at 50 and 150 percent of the nominal flow rates.

### Nomenclature (cont.)

- $T_a$  = nondimensional ambient temperature,  $T_a = t_a c_p (2C/d)^2 / (\mu_i \omega)$
- $T_j$  = nondimensional journal surface temperature  $T_c = t_c c_p (2C/d)^2 / (\mu_i \omega)$
- $T_f$  = nondimensional oil film temperature,  $T_f = t_f c_p (2C/d)^2 / (\mu_i \omega)$
- $T_p$  = nondimensional bearing temperature,  $T_p = t_p c_p (2C/d)^2 / (\mu_i \omega)$
- $U, W$  = nondimensional oil velocity components in circumferential and axial directions, respectively,  $U = 2u / (\omega d)$ ,  $W = 2w / (\omega d)$

- $Y_f$  = nondimensional radial oil film coordinate,  $Y_f = y_f / C$
- $Z$  = nondimensional axial coordinate,  $Z = 2z / L$
- $\alpha$  = heat transfer coefficient
- $\delta$  = local pad distortion
- $\lambda$  = hot oil carry over factor (or mixing coefficient)
- $\lambda_t$  = coefficient of thermal expansion
- $\mu$  = local oil viscosity
- $\mu_i$  = inlet oil viscosity
- $\rho$  = oil density
- $\omega$  = shaft angular speed
- $\Delta$  = nondimensional local pad deflection,  $\Delta = \delta / C$

- $\Delta T_p$  = local, nondimensional temperature difference across pad
- $\Lambda$  = reciprocal of Peclet number,  $\Lambda = k_o / (\omega \rho C^2)$
- $\Lambda_B, \Lambda_S, \Lambda_T$  = coefficients in pad deflection Eq. (22), see relationship (23)
- $\theta$  = time
- $\psi$  = angular coordinate
- $\psi_1$  = pad leading edge angular coordinate
- $\psi_2$  = pad trailing edge angular coordinate
- $\psi_e$  = angular coordinate: end of pressure zone
- $\psi_{piv}^{(i)}$  = angular pivot location of  $i$ th pad

Table 1 Nominal oil flow rates ( $10^{-4} \text{ m}^3/\text{s}$ )

Load, N	Shaft speed, rpm					
	1800	3600	5000	9000	12000	16500
1300	0.15	0.39	0.61	1.37	2.11	3.60
5200	0.21	0.52	0.76	1.56	2.32	3.81
10350	0.28	0.66	0.93	1.82	2.63	4.21
11200	0.29	0.65	0.95	1.85	2.67	4.27

### Computer Model

Thermohydrodynamic models of the conventional and LEG bearing designs were used to evaluate their steady state performance. These models calculate the pressure, temperature, and film thickness distributions at each pad, after accounting for thermal and elastic distortion of the bearing pads, and cross film variations in temperature (and viscosity).

**Reynolds' Equation.** The pressure distribution in the oil film is calculated from the following nondimensional form of the Reynolds' equation in cylindrical coordinates (Dowson, 1962 and Hakanson, 1965):

$$\frac{\partial^2 P}{\partial \psi^2} + \left[ 3 \frac{\partial H}{\partial \psi} + \frac{d}{d\psi} \left( \int_0^1 S_1 dY_f \right) \right] \frac{\partial P}{\partial Z} + \left( \frac{d}{L} \right)^2 \frac{\partial^2 P}{\partial Z^2} = \frac{1}{H^3} \int_0^1 S_1 dY_f \left[ \frac{\partial H}{\partial \psi} \left( \int_0^1 S_2 dY_f - 1 \right) + H \frac{\partial}{\partial \psi} \left( \int_0^1 S_2 dY_f \right) - \frac{\partial H}{\omega \partial \theta} \right] \quad (8)$$

where

$$S_1 = \int_0^{Y_f} \frac{Y_f}{M} dY_f - \frac{\int_0^{Y_f} Y_f dY_f}{\int_0^{Y_f} \frac{1}{M} dY_f} \int_0^{Y_f} \frac{1}{M} dY_f, \quad S_2 = \frac{\int_0^{Y_f} \frac{1}{M} dY_f}{\int_0^1 \frac{1}{M} dY_f} \quad (9)$$

The coordinate system is shown in Fig. 4.

For an uncavitated film, Eq. (8) is solved assuming that  $p$

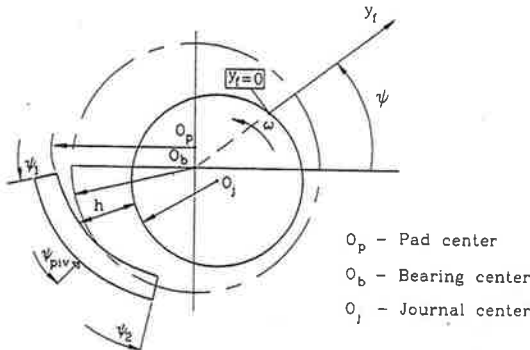


Fig. 4 Coordinate system

$= P = 0$  at all boundaries. For a cavitated film, the Swift-Stieber boundary condition is assumed, i.e.,

$$P = \frac{\partial P}{\partial \psi} = 0 \quad (11)$$

at the end of the pressure zone.

**Energy Equation.** The temperature distribution in the oil film is governed by the energy equation. This equation takes account of heat convection in the circumferential direction and heat conduction across the oil film (Dmochowski, 1981), i.e.,

$$U_{av} \frac{\partial T_f}{\partial \psi} - \frac{\Lambda}{H^2} \frac{\partial^2 T_f}{\partial Y_f^2} = \frac{M}{H^2} \left[ \left( \frac{\partial U}{\partial Y_f} \right)_{av}^2 + \left( \frac{\partial W}{\partial Y_f} \right)_{av}^2 \right] \quad (12)$$

(see Fig. 4 for coordinate system).

The values of  $U$ ,  $\partial U / \partial Y_f$ ,  $\partial W / \partial Y_f$  are averaged in the axial direction because, as with the Reynolds' equation, the oil temperature in the axial direction is assumed to be constant.

The boundary conditions for the energy equation are determined by consideration of the following:

(a) The journal surface temperature. This is assumed to be equal to the average of all the pad surface temperature distributions (Dowson et al., 1967), i.e.,

$$(T_f)_{Y_f=0} = T_j = \frac{1}{2\pi} \sum_i \int_{\psi_1^{(i)}}^{\psi_2^{(i)}} (T_p)_{R=d}^{(i)} d\psi \quad (13)$$

(b) Temperature distribution at the pad surface, i.e.,

$$T_f(\psi)_{Y_f=h}^{(i)} = T_p(\psi)_{R=d}^{(i)} \quad (14)$$

Boundary conditions (a) and (b) are illustrated in Fig. 5.

(c) Oil film temperature at the pad leading edge. This is assumed to be constant in the radial direction (but variable in other locations of the film).

Previous attempts to calculate the temperature of the oil at the pad leading edge (Eqs. (1) to (7)) were based on simplified theoretical analyses and experimental data, and were subject to a certain amount of error. This caused the authors to consider using simpler models which would consider mixing of the hot and cold oil streams at the leading edge of the oil film. This avoids the use of empirical relationships and gives, as it will be shown later, theoretical results which are in good agreement with the test data. In the case of the conventional bearing, it is assumed that all flow  $q_2$  (at temperature  $t_2$ ) from the trailing edge of one pad enters the oil film of the next adjacent pad (the limitation being that a maximum of 90 percent of  $q_1$  can be carried over). In Eq. (3), this assumption implies that  $\lambda = 0$ . This leads to the following simple heat balance equation:

$$t_1 = \frac{(q_1 - q_2)t_1 + q_2 t_2}{q_1} \quad (15)$$

In the case of the LEG bearing, the addition of the oil distribution groove has a significant effect on both the oil flow

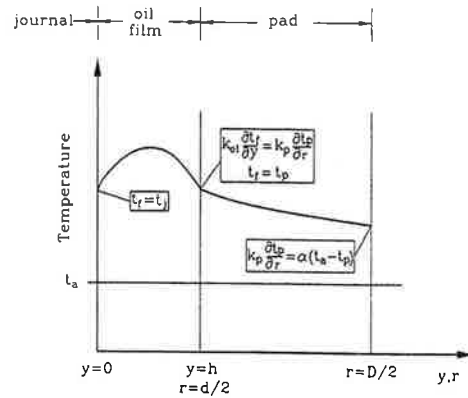


Fig. 5 Boundary conditions for the energy and heat transfer equations

and heat exchange at the leading edge of the film. The authors assumed, therefore, that all cold oil entering the leading edge groove would be pulled, by the action of the rotating shaft, into the oil film. This assumption can lead to significant reductions in both the amount of hot oil carried over from the previous pad and the oil temperature at the leading edge of the next pad. Thus:

$$t_1 = \frac{q_1 t_1 + (q_1 - q_1) t_2}{q_1} \quad (16)$$

**Heat Transfer Equation.** The pad is assumed to be part of a cylinder of inner diameter  $d$ , outer diameter  $D$  and width  $L$ . If the temperature in the axial direction is assumed constant, heat transfer through the pad is governed by the Laplace equation, i.e.,

$$\frac{\partial^2 T_p}{\partial R^2} + \frac{1}{R} \frac{\partial T_p}{\partial R} + \frac{1}{R^2} \frac{\partial^2 T_p}{\partial \psi^2} = 0 \quad (17)$$

Boundary conditions (see Fig. 5) correspond to:

(a) equality of heat flux at the pad inner surfaces, i.e.,

$$\left( \frac{\partial T_p}{\partial R} \right)_{R=1} = \frac{k_{ol}}{k_p} \frac{d}{2C} \frac{1}{H} \left( \frac{\partial T_f}{\partial Y_f} \right)_{Y_f=1} \quad (18)$$

(b) convection of heat from all pad surfaces, i.e.,

$$\left( \frac{\partial T_p}{\partial R} \right)_{R=D/d} + Nu (T_p)_{R=D/d} = Nu T_a \quad (19)$$

at the pad outer surface, and

$$\left( \frac{\partial T_p}{\partial \psi} \right)_{\psi=\psi_{1,2}} + Nu (T_p)_{\psi=\psi_{1,2}} = Nu T_a \quad (20)$$

at the ends of the pad.

In a cavitated region of the oil film, the heat flux at the inner surface of the pad is corrected by assuming that there is only a single stream of oil. Outside of this stream, it is assumed that there is no heat exchange whatsoever. Thus:

$$\left( \frac{\partial T_p}{\partial R} \right)_{R=1} = \frac{H(\psi_e)}{H(\psi)} \frac{\int_0^1 U_{av}(\psi_e) dY_f}{\int_0^1 U_{av}(\psi) dY_f} \frac{k_{ol}}{k_p} \frac{d}{2C} \frac{1}{H} \left( \frac{\partial T_f}{\partial Y_f} \right)_{Y_f=1} \quad (21)$$

Boundary conditions (14) and (18) couple together the energy and heat transfer equations, which are then solved simultaneously.

**Pad Deflection.** Pad deflection is calculated from a one dimensional equation used commonly in beam theory (Ettles,

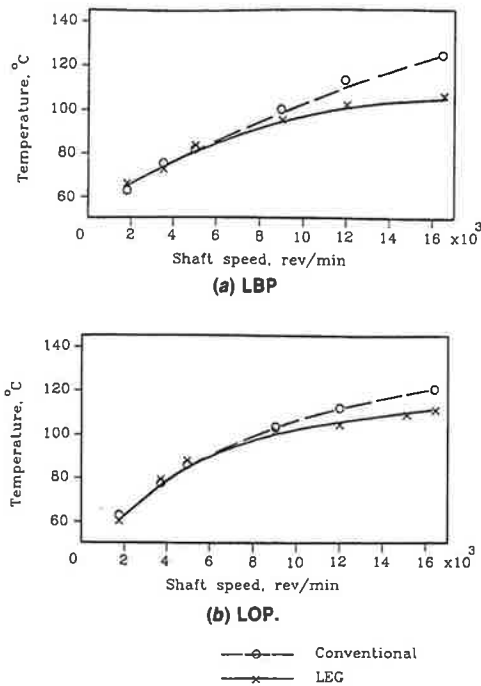


Fig. 6 Maximum pad temperature versus shaft speed. Load 11.2 kN.

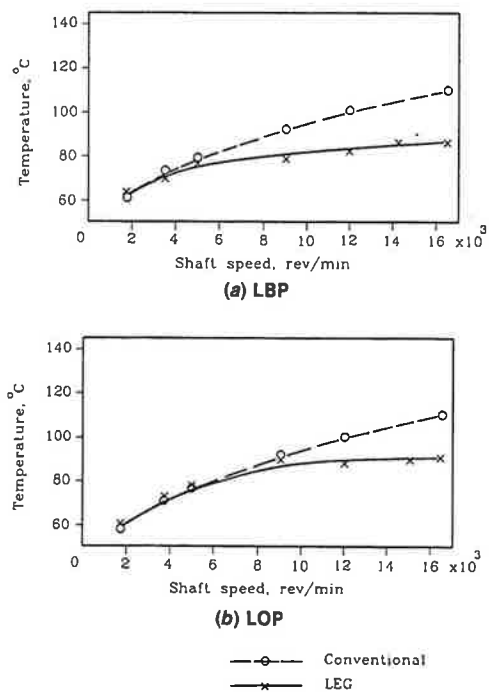


Fig. 7 Maximum pad temperature versus shaft speed. Load 5.2 kN.

1980). This equation allows for the effects of bending moment, shear force and a temperature gradient across the pad thickness, and is:

$$\frac{d^2 \Delta}{d\psi^2} = \Lambda_B \frac{g_{piv}^3}{g^3} M_b + \Lambda_S \frac{g_{piv}}{g} P_{av} + \Lambda_T \frac{g_{piv}}{g} \Delta T_p \quad (22)$$

where

$$\Lambda_B = \frac{\mu_f \omega L d^3}{8 \left(\frac{2C}{d}\right)^3 EI_{piv}} \quad \Lambda_S = \frac{\mu_f \omega d}{8 \left(\frac{2C}{d}\right)^3 G g_{piv}} \quad (23)$$

$$\Lambda_T = \frac{\mu_f \omega d \lambda_f}{2c_v \rho \left(\frac{2C}{d}\right)^3 g_{piv}} \quad (23)$$

The boundary conditions are:

$$\Delta = 0 \quad \text{and} \quad \frac{d\Delta}{d\psi} = 0 \quad \text{at} \quad \psi = \psi_{piv} \quad (24)$$

Equations (8)–(24) are solved using the finite difference method (Dmochowski, 1981). The iteration procedure, described by Brockwell and Dmochowski (1992), continues until the convergence criteria are fulfilled. For the pressure, energy and heat transfer equations, convergence is achieved if two consecutive approximations differ by less than 1 percent.

### Experimental Results

**Conventional Versus LEG Bearing Temperatures.** Figure 6(a) shows the maximum pad temperatures, plotted against shaft speed, of the conventional and LEG bearings (measured at the 95 percent location—see Fig. 2), for LBP and a load of 11.2 kN. The maximum temperature of the bearings was similar for speeds below 5000 rev/min, but at higher speeds the LEG bearing ran cooler. For example, at 16500 rev/min the maximum temperature of the LEG bearing was 103°C, compared to 123°C in the case of the conventional bearing. For LOP, the maximum temperature in both bearings was similar for shaft speeds up to 9000 rev/min, but at higher speeds the LEG bearing was again cooler. For example, at 16500 rev/min the

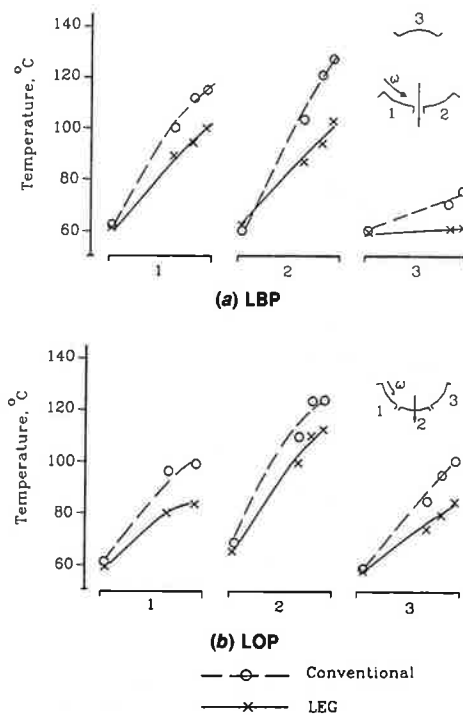


Fig. 8 Pad temperature profiles. Load 11.2 kN, shaft speed 16,500 rpm.

maximum temperature of the LEG bearing was 112°C, compared to 122°C in the case of the conventional bearing (see Fig. 6(b)). Figure 7 shows that the bearings exhibited a similar behavior with a load of 5.2 kN.

Figures 8(a) and 8(b) show measured circumferential pad temperature profiles for LBP and LOP respectively, for a shaft speed of 16500 rev/min and a load of 11.2 kN. These figures show two interesting features. Firstly, the pad leading edge temperatures of the conventional and LEG bearings are similar. Secondly, for LBP, temperature distributions on the loaded pads of the LEG bearing are similar, whereas those of the

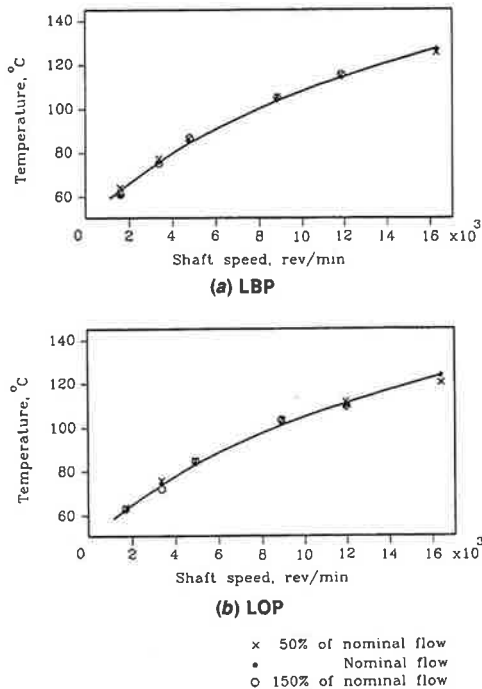


Fig. 9 Maximum pad temperature versus shaft speed. Conventional bearing, load 11.2 kN.

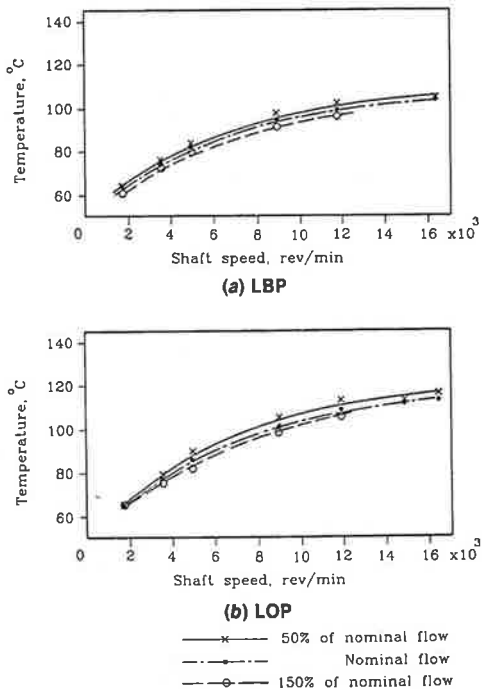


Fig. 10 Maximum pad temperature versus shaft speed. LEG bearing, load 11.2 kN.

conventional bearing are different, viz. pad #2 is hotter than pad #1.

**Effect of Oil Flow.** Tests to determine the effect of rate of oil flow on maximum bearing temperature were made by varying the flow rate between 50 and 150 percent of the nominal values (see Table 1). Figures 9 and 10 show results from the conventional and LEG bearings, respectively, for both LBP and LOP and a load of 11.2 kN. Figure 9 shows that the temperature of the conventional bearing changed by only 2C as a result of varying the flow (with higher flow rates, slightly

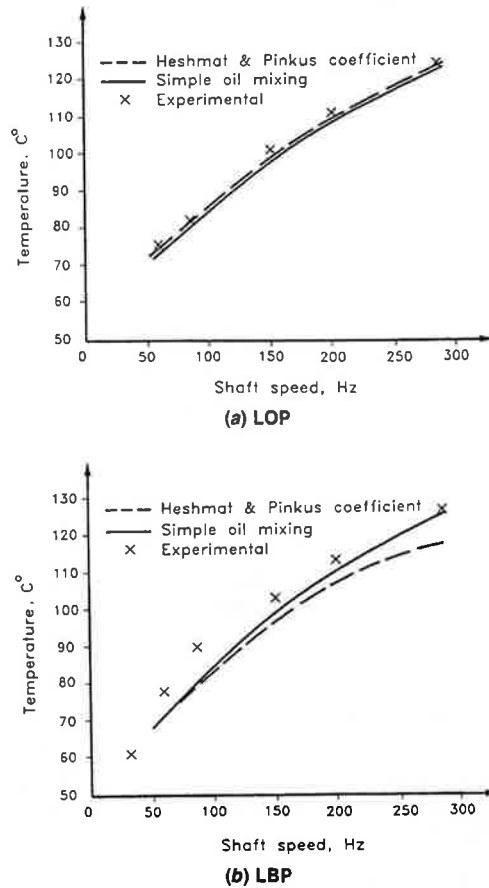


Fig. 11 Maximum pad temperature versus shaft speed. Comparison of calculated and experimental results. Conventional bearing, load 11.2 kN, LBP.

lower bearing temperatures may have been the result of increased cooling by the cold oil. However, these variations are small and within the uncertainty of the measurement). In the case of the LEG bearing (Fig. 10), the change in maximum pad temperature reached 6C when the flow rate was varied between 50 and 150 percent of the nominal flows.

### Comparison of Theoretical and Experimental Results

A comparison of test data from the conventional bearing, with results obtained from the Heshmat and Pinkus relationships (Eqs. (3) through (7)) and the author's mixing equation, are shown in Fig. 11. For LOP (Fig. 11(a)), agreement is very good. However, for LBP (Fig. 11(b)) the mixing coefficient represented by Eq. (5) underestimates the effect of hot oil carry over, particularly at higher shaft speeds. For example, at 16500 rev/min the predicted maximum pad temperature is 12C lower than the measured maximum temperature. Figure 11(b) shows also that, for this particular study, the simple mixing Eq. (15) gives better correlation with the experimental results.

Figure 12 presents a comparison of the calculated pad temperature profiles (from the simple mixing theory) with the measured results, for a speed of 16500 rev/min and a load of 11.2 kN. Figure 12(a) is for LBP, and 12(b) is for LOP. There is fairly good agreement between the calculated and measured temperatures, particularly in the vicinity of the leading and trailing edges of the pads. This leads the authors to conclude that Eqs. (15) and (16) may be used, with a reasonable degree of confidence, to predict leading edge oil temperatures in the conventional and LEG bearings, respectively. Further confirmation is to be found in Figs. 13 and 14, which show good correlation between measured and calculated maximum pad

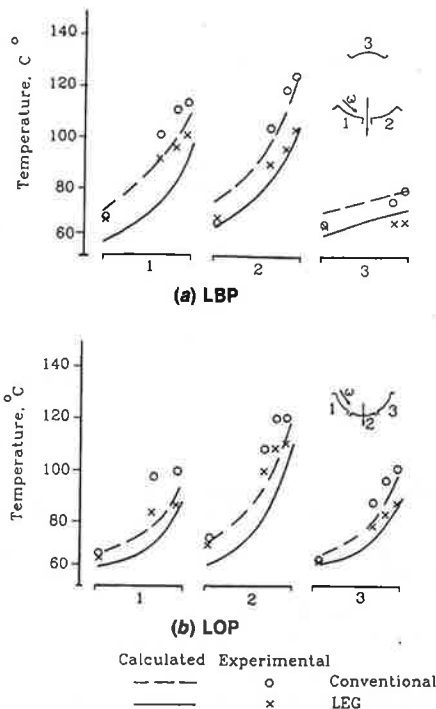


Fig. 12 Pad temperature distribution. Comparison of calculated and experimental results. Load 11.2 kN, shaft speed 16,500 rpm.

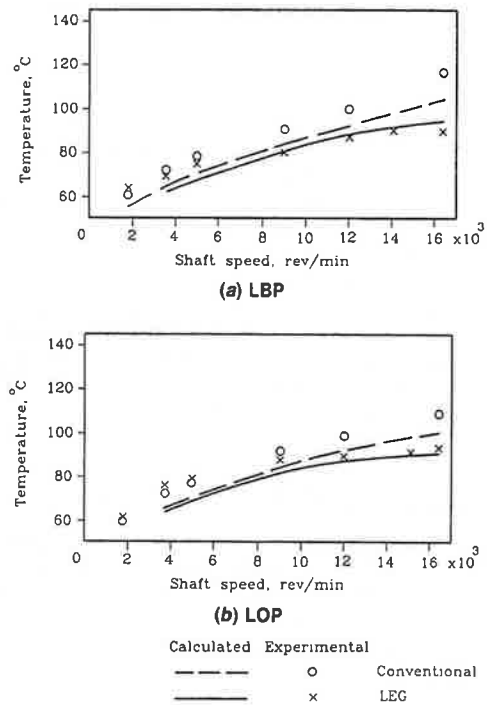


Fig. 14 Maximum pad temperature versus shaft speed. Comparison of calculated and experimental results. Load 5.2 kN.

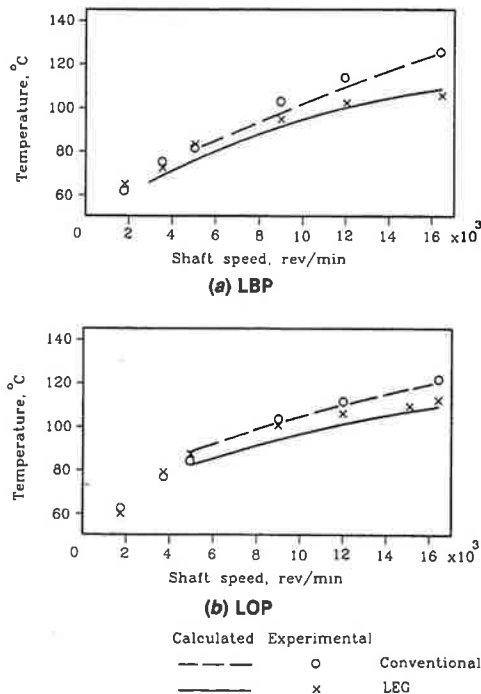


Fig. 13 Maximum pad temperature versus shaft speed. Comparison of calculated and experimental results. Load 11.2 kN.

temperatures for a range of shaft speeds, and loads of 11.2 and 5.2 kN, respectively.

### Discussion

Analyses of the conventional and LEG bearings have shown that the difference in their thermal behavior is the result of hot oil carry over between adjacent pads. In the case of the conventional bearing, a comparison of the theoretical and experimental results (Figs. 12, 13, and 14) has shown that most

hot oil leaving the trailing edge of one pad is carried over to the leading edge of the next adjacent pad. The balance comes from the cold oil supplied to the bearing. In the case of the LEG bearing, all cold oil supplied to the leading edge groove, with the exception of any side leakage from the groove, is pulled, by the action of the rotating shaft, into the oil film. (This assumption is made on the basis that the oil pressure in the leading edge groove is not sufficient to cause oil to flow in a direction opposite to that of the shaft rotation.) Hot oil carried over from the trailing edge of the previous pad provides the balance of the flow at the leading edge of the pad. As a result, hot oil carry over in the LEG bearing is reduced and this results in significantly lower pad operating temperatures when compared to those of the conventional bearing.

With regard to the similar leading edge temperatures measured on the bearings (see Fig. 8), this may be the result of heat conduction through the pad. However, a more likely explanation is that the hot and cold oil streams are not fully mixed at the leading edge of the oil film. This would confirm the earlier observations of Ettles and Cameron (1968) and Heshmat and Pinkus (1986) who postulated that a layer of hot oil adheres to the surface of the shaft, while cool oil supplied to the bearing enters the oil film at a point directly adjacent to the pad surface. Assuming that this effect occurs in both types of bearing, this would seem to be the most likely explanation for the similarity in their leading edge temperatures.

To explain the effect of oil flow rate on the thermal characteristics of the bearings, one needs to consider oil conditions at the inlet region of the pad. In the case of the conventional bearing, it was shown that a variation in the oil flow rate had little effect on bearing temperatures. That is, increasing the flow rate by 50 percent was ineffective, as indeed was a 50 percent reduction in flow. Presumably, this is because there is always sufficient cold oil in the cavity of the bearing to provide the leading edge of each pad with the right amount of "make up" flow ( $q_1$ ). The result is that bearing temperatures remain much the same, regardless of oil flow rate. However, decreasing the oil flow to the LEG bearing will result in a reduction in the amount of cool oil entering any one pad. Consequently, to make up the balance, more hot oil from the

previous pad is required and this results in higher bearing temperatures (Fig. 10).

## Conclusions

1. The leading-edge-groove bearing, when compared to the equivalent conventional bearing, has been shown to operate with lower babbitt temperatures. Theoretical analysis has shown that this is the result of feeding cool oil directly to the leading edge of the pads. This has the effect of reducing the amount of oil carried over from one pad to the next.

2. To calculate the oil temperature at the leading edge of the pads of the conventional and LEG bearings, simple "mixing" equations have been proposed. When these equations are used in full thermohydrodynamic models of the two bearing designs, theoretical results are obtained which are in good agreement with experimental data.

## Acknowledgments

The authors wish to thank the National Research Council Canada and Kingsbury, Inc. for permission to publish this paper. Special thanks go to Mr. D. Kleinbub, and other staff of the NRC Tribology and Mechanics Laboratory, for their help in carrying out this study.

## References

Brockwell, K., and Dmochowski, W., 1992, "Thermal Effects in the Tilting Pad Journal Bearing," *Journal of Physics, D: Applied Physics*, Vol. 25, pp. 384-392.

Dmochowski, W., 1981, "A Numerical Method for Calculating Journal Bearing Steady State Characteristics Including Thermal Effects," Ph.D. thesis, Institute of Fluid Flow Machinery, Gdansk, Poland.

Dowson, D., 1962, "A Generalized Reynolds' Equation for Fluid Film Lubrication," *International Journal of Mechanical Sciences*, Vol. 4, pp. 159-170.

Dowson, D., Hudson, J. D., Hunter, B., and March, C. N., 1967, "An Experimental Investigation of Temperature Effect in Journal Bearings," *Journal Bearing for Reciprocating and Turbo Machinery, Proceedings of the Institution of Mechanical Engineers 1966-67*, Vol. 181, Part 3B, pp. 70-80.

Ettles, C., and Cameron, A., 1968, "Consideration of Flow Across a Bearing Groove," *ASME JOURNAL OF LUBRICATION ENGINEERING*, Vol. 90, pp. 313-319.

Ettles, C., 1968, "Solutions for Flow in a Bearing Groove," *Tribology Convention, Proceedings IMechE 1967-1968*, Vol. 182, Part 3N, pp. 120-131.

Ettles, C., 1970, "Hot Oil Carry-Over in Thrust Bearings," *Proceedings IMechE 1969-1970*, Vol. 184, Part 3L, pp. 75-81.

Ettles, C.M.McC., and Advani, S., 1980, "The Control of Thermal and Elastic Effects in Thrust Bearings," *Thermal Effects in Tribology, Proceedings of the 6th Leeds-Lyon Symposium*, D. Dowson et al., eds., Mechanical Engineering Publications Ltd., London, 1980, pp. 105-116.

Ettles, C.M.McC., 1980, "The Analysis and Performance of Pivoted Pad Journal Bearings Considering Thermal and Elastic Effects," *ASME JOURNAL OF LUBRICATION ENGINEERING*, Vol. 102, pp. 182-192.

Hakanson, B., 1965, "The Journal Bearing Considering Variable Viscosity," *Transactions of Chalmers University of Technology*, Gothenburg, Sweden, No. 298.

Heshmat, H., and Pinkus, O., 1986, "Mixing Inlet Temperatures in Hydrodynamic Bearings," *ASME JOURNAL OF LUBRICATION ENGINEERING*, Vol. 108, pp. 231-248.

Mikula, A. M., 1988, "Further Test Results of the Leading-Edge-Groove (LEG) Tilting Pad Thrust Bearing," *ASME JOURNAL OF LUBRICATION ENGINEERING*, Vol. 110, pp. 174-180.

Mitsui, J., Hori, Y., and Tanaka, M., 1983, "Thermohydrodynamic Analysis of Cooling Effect of Supply Oil in Circular Journal Bearing," *ASME JOURNAL OF LUBRICATION ENGINEERING*, Vol. 105, pp. 414-420.

Vohr, J. H., 1981, "Prediction of the Operating Temperature of Thrust Bearings," *ASME JOURNAL OF LUBRICATION ENGINEERING*, Vol. 103, pp. 97-106.